A 100 Myr history of the carbon cycle based on the 400 kyr cycle in marine δ 13 C benthic records

Didier Paillard, Yannick Donnadieu

AGU PUBLICATIONS

Paleoceanography

RESEARCH ARTICLE
10.1002/2014PA002693

Key Points:
- Continuous robust information on past carbon cycle
- Simple methodology consistent with Cenozoic CO_2 data
- Original use of readily available isotopic data

Supporting Information:
- Readme
- Table S1

Correspondence to:
D. Paillard,
didier.paillard@lsce.ipsl.fr

Citation:
Paillard, D., and Y. Donnadieu (2014), A 100 Myr history of the carbon cycle based on the 400 kyr cycle in marine $\delta^{13}C$ benthic records, *Paleoceanography*, *29*, 1249–1255, doi:10.1002/2014PA002693.

Received 3 JUL 2014
Accepted 31 OCT 2014
Accepted article online 4 NOV 2014
Published online 20 DEC 2014

A 100 Myr history of the carbon cycle based on the 400 kyr cycle in marine $\delta^{13}C$ benthic records

Didier Paillard[1] and Yannick Donnadieu[1]

[1]Laboratoire des Sciences du Climat et de l'Environnement (CEA/CNRS/UVSQ-IPSL), Gif-sur-Yvette, France

Abstract Documenting the past coevolution of Earth temperatures and of the carbon cycle is of paramount importance for our understanding of climate dynamics. Atmospheric CO_2 is well constrained over the last million years through direct measurements in air bubbles from Antarctic ice cores. For older times, many different and sometimes conflicting proxies have been suggested. Here we provide a new methodology to constrain the carbon cycle in the past, based on marine benthic $\delta^{13}C$ records. Marine $\delta^{13}C$ data are recording a persistent 400 kyr cycle, with an amplitude primarily linked to the total amount of carbon in the ocean, or dissolved inorganic carbon (DIC). By extracting this amplitude from published records, we obtain a new strong constraint on the 100 Myr history of Earth's carbon cycle. The obtained Cenozoic evolution of DIC is in surprisingly in a good agreement with existing reconstructions of pCO_2, suggesting that pCO_2 is mostly driven by DIC changes over this period. In contrast, we find no strong decreasing trend in DIC between the Cretaceous and the Cenozoic, suggesting that Cretaceous atmospheric pCO_2 levels were limited, and high temperatures at this time should be explained by other mechanisms. Alternatively, high Cretaceous atmospheric pCO_2 could occur as a consequence of changes in oceanic chemistry but not carbon content.

1. Introduction

Reconstructing the Earth's carbon cycle in the geological past is a difficult task since evidence is usually indirect and sparse. Most studies have been focused on estimating atmospheric CO_2 partial pressure (pCO_2) since this is a critical climatic forcing. But the size of the atmospheric reservoir is only a few percent of the oceanic one, and pCO_2 is, on long time scales, at equilibrium with the ocean carbon content and ocean chemistry. It is therefore quite relevant to provide estimations of the oceanic carbon pool, i.e.,the concentration in dissolved inorganic carbon (DIC). To our knowledge, this has never been attempted before. Furthermore, this may have several advantages over pCO_2 estimates. Indeed, available pCO_2 proxies are based on boron isotopes, on $\delta^{13}C$ from phytoplankton, paleosols or liverworts, or on paleobotanical evidences like stomatal indices [*Beerling and Royer*, 2011; *Royer*, 2006]. The associated uncertainties remain huge [e.g., *Pagani et al*., 2005; *Zhang et al*., 2013]. The stomatal index method relies on present-day correlations between stomatal indices and pCO_2 for living plants [*Retallack*, 2001]. Such relationships are applied to the geological past and to pCO_2 levels far beyond any observed values. Similarly, paleosol pCO_2 estimates are systematically higher than the ones based on stomatal index [*Royer*, 2006; *Fletcher et al*., 2008]. Nevertheless, a recent study [*Breecker et al*., 2010] suggests that lower paleosol pCO_2 estimates are obtained when accounting for reduced CO_2 levels in soils, a parameter that strongly depends on hydrology, temperature, and vegetation, which cannot easily be defined for past environments [*Gulbranson et al*., 2011]. More generally, stomatal or paleosol data are affected by individual or geographical variability, which leads to large uncertainties and possible difficulties in their interpretation.

In contrast, in paleoceanography, it is usually assumed that benthic (i.e., deep dwelling) foraminifera are recording geochemical properties that represent first-order global average values. Based on these premises, benthic $\delta^{18}O$ and $\delta^{13}C$ isotopic stacks have been constructed for the Cenozoic [*Zachos et al*., 2001] and for the Late Mesozoic [*Friedrich et al*., 2012]. These reconstructions provide robust information on global ocean properties, and it would be desirable to derive quantitative information on the carbon cycle from this type of data. Here we suggest a new method to better constrain the carbon content of the ocean-atmosphere system using the 400 kyr cycles in deep-marine $\delta^{13}C$ records.

An intriguing feature of long-term benthic $\delta^{13}C$ records is the existence of a persistent 400 kyr periodicity. A clear signal has been identified during the Oligocene [*Pälike et al*., 2006], the Eocene [*Sexton et al*., 2011], the Miocene [*Billups et al*., 2004], and also during the most recent time periods [*Wang et al*., 2010]. This astronomical periodicity is the most stable one through geological times [*Laskar et al*., 2004] and is a primary target for cyclostratigraphy for the early Cenozoic, the Mesozoic, and beyond [*Hinnov and Ogg*, 2007]. This $\delta^{13}C$ oscillation reflects periodic changes in the sources and sinks of oceanic and atmospheric carbon, whose mechanisms are still unclear. There is a strong suspicion that the monsoon has an active role in controlling carbon sinks on this time scale, either through inorganic carbon via continental weathering [*Pälike et al*., 2006] or through organic carbon via carbon burial or nutrient supply [*Wang et al*., 2004]. Some box model experiments [*Russon et al*., 2010] suggest that the amplitude and phase patterns observed over the Pliocene-Pleistocene are more easily explained through changes in marine productivity or rain ratio, as suggested by some data [*Rickaby et al*., 2007]. Whatever the mechanisms, the $\delta^{13}C$ signature of the surface reservoirs will be more easily affected if the amount of carbon is small. The surface carbon reservoir includes the ocean, the atmosphere, and the biosphere, with, respectively, about 38,000 PgC, 600 PgC, and 2000 PgC during preindustrial times [e.g., *Intergovernmental Panel on Climate Change*, 2013]. We will therefore consider in the following that the total surface carbon is almost equivalent to the oceanic carbon or DIC. Assuming a constant external periodic 400 kyr forcing linked to some astronomical influence on the carbon system, the amplitude of the $\delta^{13}C$ oscillations should therefore be inversely related to the size of the exospheric carbon pool. This is the conceptual foundation of our method.

The configuration of continents, oceans, or mountains does change considerably over the last 100 Myr, and the 400 kyr carbon oscillator might have been amplified or dampened at some time periods. For instance, if these oscillations are linked to continental weathering, they should be modulated by orogeny or by the location of low-latitude continental masses [*Goddéris et al*., 2014]. If linked to marine productivity or rain ratio, they should also be modulated by nutrient supply or ecological shifts. Without knowing the mechanisms, it is difficult to discuss how the Earth's sensitivity to the 400 kyr forcing might change. The fact that these oscillations persist in widely different geographic and climatic contexts is indicative of the robustness of the processes involved. For instance, orbital scale evolution of the tropical watersheds that are linked to the monsoonal systems has been demonstrated to be a robust feature with strong similarities between the Holocene and the Cretaceous [*Flögel et al*., 2008]. The persistence of these features prompts us to assume in the following that this carbon oscillator remains stable and that the corresponding amplitude of $\delta^{13}C$ oscillations can be interpreted mostly in terms of carbon reservoir size. This is of course a critical assumption that needs to be assessed more precisely in future works.

2. Methodology

We are using benthic isotopic $\delta^{13}C$ records that have already been selected to build a Cenozoic stack [*Zachos et al*., 2001] and a Late Cretaceous one [*Friedrich et al*., 2012]. Each individual record from these two stacks was filtered at 400 kyr (Gaussian filter at 2.5 ± BW Myr^{-1}; BW = bandwidth) and the amplitude (AMPL) was extracted through a Hilbert transform. An important parameter in this analysis is the bandwidth (BW) of the filter. Indeed, a narrow bandwidth will be very selective and will keep only frequencies near 2.5 Myr^{-1} that remain stable over a rather long duration, scaling as 1/BW. It will thus provide a smoother and more robust result, since the corresponding estimations will be based on a larger amount of data points, or "time window." But it may be too selective and may not accommodate for errors in the absolute time scales of the record or for possible rapid changes in amplitude or phase of the 400 kyr signal in $\delta^{13}C$ records. Conversely, a large bandwidth (i.e., a small time window) will provide more detailed but also less robust results. Stated alternatively, one cannot sharply characterize a signal simultaneously in the time and in the frequency domains: this is referred to as the Gabor limit in signal processing or as the Heisenberg uncertainty principle in quantum mechanics.

We used different values of BW, ranging from 0.1 to 1.0 Myr^{-1}. The computed 400 kyr amplitudes are selected whenever the data point density in the record is sufficiently high. Indeed, when the data are too sparse, it is not possible to extract a significant 400 kyr component in the record, and the resulting amplitude becomes very low or zero. The Nyquist criterion requires at least two data points per cycle, which corresponds to a minimum density of 5 samples per million years. In order to be conservative, we have used a minimum

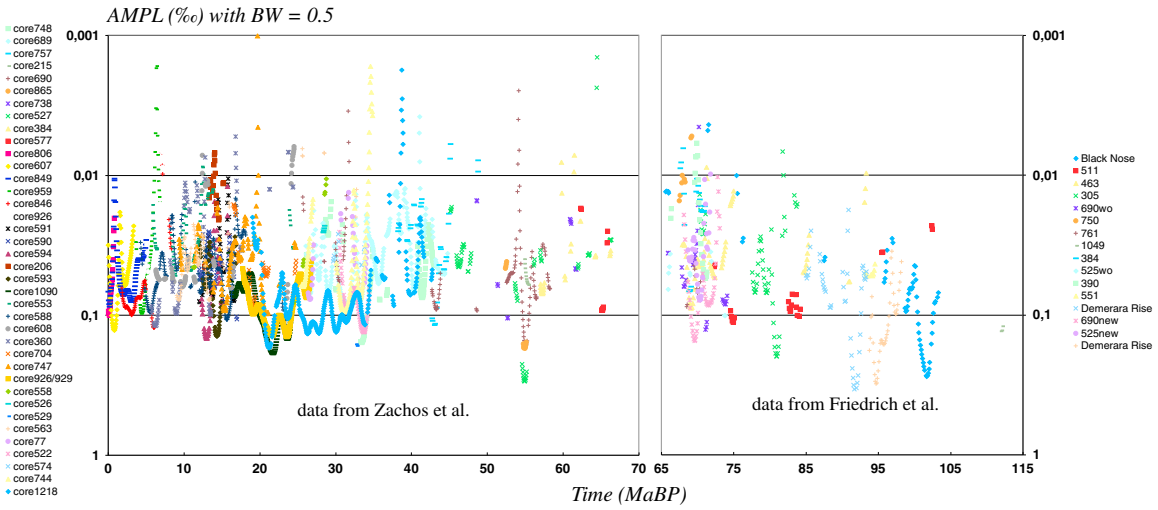

Figure 1. Estimations of the amplitude of the 400 kyr cycle in individual $\delta^{13}C$ benthic records from the Cenozoic stack (8) and the Late Cretaceous one (9) using a bandwidth BW = 0.5.

density of 10 samples per million years as a selection criterion. For example, the computed amplitudes for BW = 0.5 (i.e., about a 2 Myr windowing) are shown in Figure 1 for individual cores of each data stack. These values are then aggregated in a sliding 2 Myr window to provide a mean value and a standard deviation, assuming a lognormal distribution. The resulting estimations of the $\delta^{13}C$ 400 kyr amplitude (AMPL) are shown in Figures 2a and 2b for BW = (0.1, 0.3, 0.5, and 1.0). As expected, the amplitude is smaller for a narrow bandwidth and larger for a wider one. The total carbon content in surface reservoirs R_{DIC} is computed as $R_{DIC} = AMPL_0/AMPL$ to normalize it to the estimated present-day value $AMPL_0$. This represents, to the first order, the carbon content of the ocean or dissolved inorganic carbon (DIC). The Cenozoic and the Cretaceous data have been processed separately, thus providing two independent reconstructions, based on different cores. They provide almost identical results in their overlapping time interval, at about 67 Ma, which indicates that our methodology is robust. The results obtained using different bandwidths are generally consistent, except when the data density is small, as can be seen in Figure 2.

3. Results and Discussion

3.1. Comparing With pCO_2 Proxies

In order for R_{DIC} to reflect atmospheric pCO_2, it would be necessary that the ocean-atmosphere partition remains constant. This is highly unlikely. For instance, assuming a constant oceanic CO_3^{2-} concentration (i.e., accounting for carbonate compensation with fixed Ca^{2+} levels), alkalinity changes should be roughly equal to DIC changes. In this case, $R_{DIC} = 2$ corresponds roughly to $pCO_2 = 4 \times$ present-day atmospheric level (4 PAL), and $R_{DIC} = 3$ corresponds to $pCO_2 = 9$ PAL [see, e.g., *Kump and Arthur*, 1999]. Such an indicative scaling is represented in Figure 3 to compare our results to previously published estimations of atmospheric CO_2.

3.2. Cenozoic Results

The general shape of R_{DIC} compares favorably with CO_2 proxies, although some systematic differences are also obvious. We observe larger amounts of carbon during the Eocene, with values in the range of 2X to 3X present-day values (i.e., Earth surface carbon = 80,000 to 120,000 PgC). The Oligocene values are consistently close to or lower than today and the mid-Miocene values in the range of 1X to 1.5X present-day values. This is very consistent with most CO_2 proxies and also with the climatic evolution over this time period [*Beerling and Royer*, 2011].

Interestingly, while R_{DIC} values are quite high during the early Paleocene, the late Paleocene carbon values are relatively low, between 1 and 2 times the current carbon content. Obviously, short-lived excursion in atmospheric pCO_2 like the Paleocene-Eocene thermal maximum (PETM event at 55 Ma) cannot be detected

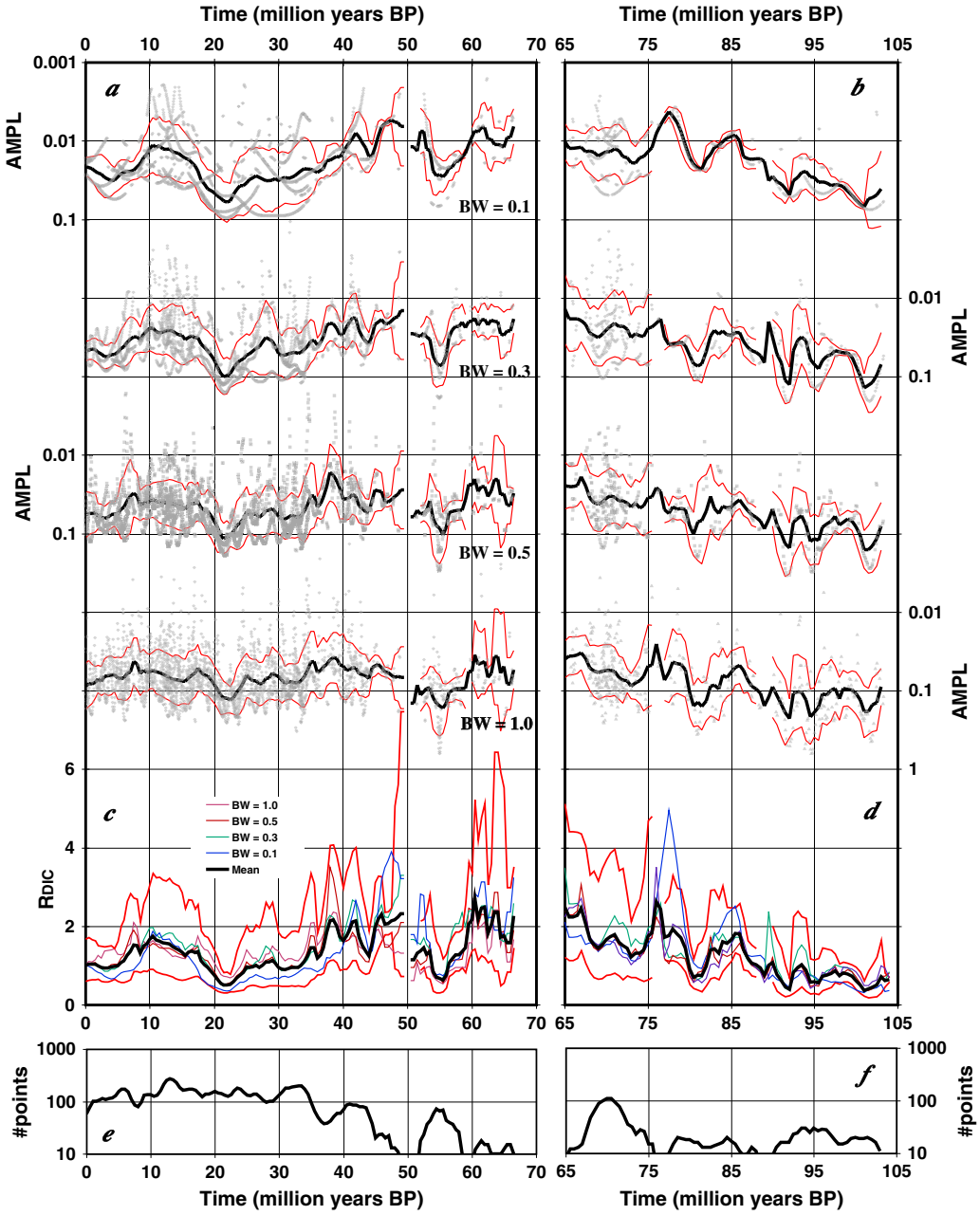

Figure 2. (a and b) The grey dots are as in Figure 1 for different bandwidth values. These individual amplitudes are then averaged in a 2 Myr sliding window to provide a mean value (black line) and a standard deviation (red lines). (c and d) The estimations thus obtained (thin colored curves for each BW) are pooled together to provide a mean estimation (black line) and a pooled standard deviation (red lines). (e and f) Number of points used in the 2 Myr sliding window.

with our tool, since AMPL is reconstructed at a multimillion year resolution only. However, our low oceanic carbon content estimated during the late Paleocene has interesting implications for the PETM story. Indeed, as noted earlier [*Pagani et al.*, 2006], the size of the carbon perturbation necessary to explain the PETM temperature excursion will be more easily accounted for in a low pCO_2 context.

Between the Eocene and Oligocene, the decreasing R_{DIC} trend occurs in two abrupt steps at about 38 Ma and about 34 Ma. Another such abrupt decrease is also present at about 24 Ma. These last two steps correspond closely to the Eocene/Oligocene and the Oligocene/Miocene boundaries and have already been identified as abrupt decreases in pCO_2 proxies [*Pagani et al.*, 2005].

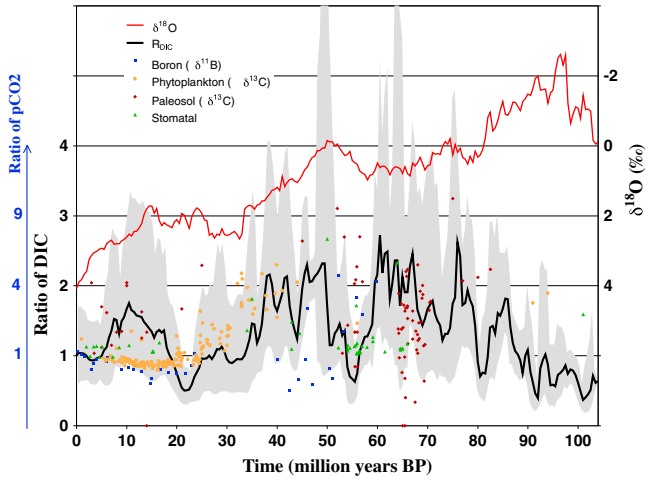

Figure 3. The $\delta^{18}O$ stack records (8 and 9) (red) are usually interpreted as representing a cooling trend over the last 100 Myr. Our mean estimation of R_{DIC} (black), with its dispersion in grey shading (cf. Figures 2c and 2d). The colored dots are proxy estimations (2) of pCO_2 using the blue scaling on the left (i.e., assuming that DIC changes are accompanied by equivalent changes in ocean alkalinity).

Over the last few million years, the $\delta^{13}C$ variability is shifted toward a 500 kyr oscillation [*Wang et al.*, 2004, 2010]. Consequently, AMPL decreases when using a narrow filter (BW = 0.1). An increasing trend in AMPL (decrease in R_{DIC}) is found with BW = 1.0 and is in better agreement with recently published data [*Seki et al.*, 2010; *Pagani et al.*, 2010; *Hönisch et al.*, 2009]. In agreement with two recent studies based on modeling [*Lefebvre et al.*, 2013] and on indirect proxy method [*Bolton and Stoll*, 2013], we found R_{DIC} values near 1.5 (which can be interpreted as pCO_2~2 PAL) during the middle Miocene and that after about 15 Ma, atmospheric pCO_2 decreases until the Pliocene with a major drop between 5 and 10 Ma [*Bolton and Stoll*, 2013]. Our rather simple methodology is therefore able to capture many features than have been reported recently concerning the evolution of the carbon cycle during the Cenozoic, although there are some differences with existing proxies of pCO_2, like the significantly lower levels found at about 23 Ma.

3.3. Cretaceous Results

During the Cretaceous, temperatures are believed to be significantly higher than today [*Littler et al.*, 2011; *Pucéat et al.*, 2007], something which is usually attributed to much higher pCO_2 levels. It is worth emphasizing that there are few proxy data for pCO_2 during this time period and that these data are not indicating extremely high levels [*Franks et al.*, 2014]. Our results demonstrate that the size of the $\delta^{13}C$ oscillation was about the same as today in the mid-Cretaceous. The amount of $\delta^{13}C$ data is reduced during this time period as well as during the early Cenozoic, and the precise estimation of R_{DIC} might be less robust. But we still detect, at least during some time intervals, a clear sizable oscillation. A poor signal would on the contrary lead to an underestimation of the 400 kyr amplitude and an overestimation of R_{DIC}. This is not the case here. These sizable oscillations are extremely difficult to explain if there were several times more carbon on Earth during this period: either the $\delta^{13}C$ signal should be considerably amplified or the 400 kyr climatic forcing should be several times larger than today through, for instance, considerably more intense monsoon systems. This seems to contradict the available records [*Flögel et al.*, 2008]. Our analysis therefore strongly suggests that the size of the surface carbon reservoir did not exhibit a significant trend over the last 100 Myr and remained mostly in the range of 40,000–100,000 PgC. But other changes in the chemistry of the ocean may also have an important role on pCO_2. Indeed, it was demonstrated [*Lowenstein et al.*, 2001] that the Mg/Ca ocean ratio was significantly smaller in Cretaceous time, due probably both to increased levels of Ca^{2+} and decreased levels of Mg^{2+}. Increased levels of Ca^{2+} by a factor of 3 to 4, as suggested by the data [*Hönisch et al.*, 2012], would decrease CO_3^{2-} concentrations and increase pCO_2 roughly in the same proportion (i.e., 3 to 4 PAL assuming a constant $R_{DIC} = 1$). Furthermore, decreased levels of Mg^{2+} would favor carbonate precipitation as calcite in contrast to present day, where aragonite is favored [*Sandberg*, 1983]. Carbonate precipitation is easier in a calcite sea, and CO_3^{2-} concentration would be even lower, thus amplifying the increase in pCO_2. But pCO_2 levels much larger than 3X or 4X present-day levels are very difficult to explain through changes in Mg/Ca only. Our analysis suggests that, during the mid-Cretaceous, atmospheric pCO_2 changes alone might not be able to account for very high temperatures. This is consistent with CO_2 proxies implying that a CO_2 content is only 2.3–4 times higher than present for the Albian-Cenomanian time periods [*Passalia*, 2009].

4. Conclusions

In summary, we are proposing a new way to constrain the carbon cycle in the past. The major features of our analysis are in broad agreement with other proxies of atmospheric CO_2 over the Cenozoic [*Beerling and Royer*, 2011]. This suggests that pCO_2 changes were mostly linked to changes in the carbon content of the ocean-atmosphere reservoirs over this time period. But we found no long-term 100 Myr trend between the Cretaceous and the Cenozoic. This implies that a putative pCO_2 decrease over this time scale should mostly be driven by changes in ocean carbonate chemistry not in total carbon content. This puts severe limitations on the maximum possible pCO_2 levels during the Cretaceous. This also questions the sensitivity of current climate models that have difficulties to simulate a warm Cretaceous climate without extremely high CO_2 values.

Acknowledgments

The data used here can be found at http://hurricane.ncdc.noaa.gov/pls/paleox/ f?p = 519:1:::::P1_STUDY_ID:8674 for the *Zachos et al.* [2001] stack and as item 2012043 in the GSA repository (http://www.geosociety.org/pubs/drpint.htm) for the *Friedrich et al.* [2012] stack. We thank O. Friedrich for providing the Cretaceous data and Y. Goddéris for the helpful discussions, as well as Lee Kump and two anonymous reviewers for their helpful comments and suggestions.

References

Beerling, D., and D. Royer (2011), Convergent Cenozoic CO_2 history, *Nat. Geosci.*, *4*, 418–420.

Billups, K., H. Pälike, J. Channell, J. Zachos, and N. Shackleton (2004), Astronomic calibration of the late Oligocene through early Miocene geomagnetic polarity time scale, *Earth Planet. Sci. Lett.*, *224*, 33–44.

Bolton, C., and H. Stoll (2013), Late Miocene threshold response of marine algae to carbon dioxide limitation, *Nature*, *500*, 558–562.

Breecker, D. O., Z. D. Sharp, and L. D. McPhaden (2010), Atmospheric CO_2 concentrations during ancient greenhouse climates were similar to those predicted for A.D. 2100, *Proc. Natl. Acad. Sci. U.S.A.*, *107*, 576–580.

Fletcher, B., S. Brentnall, C. Anderson, R. Berner, and D. Beerling (2008), Atmospheric carbon dioxide linked with Mesozoic and early Cenozoic climate change, *Nat. Geosci.*, *1*, 43–48.

Flögel, S., B. Beckmann, P. Hofmann, A. Bornemann, T. Westerhold, R. D. Norris, C. Dullo, and T. Wagner (2008), Evolution of tropical watersheds and continental hydrology during the Late Cretaceous greenhouse; impact on marine carbon burial and possible implications for the future, *Earth Planet. Sci. Lett.*, *274*, 1–13.

Franks, P. J., D. L. Royer, D. J. Beerling, P. K. Van de Water, D. J. Cantrill, M. M. Barbour, and J. A. Berry (2014), New constraints on atmospheric CO_2 concentration for the Phanerozoic, *Geophys. Res. Lett.*, *41*, 4685–4694, doi:10.1002/2014GL060457.

Friedrich, O., R. Norris, and J. Erbacher (2012), Evolution of middle to Late Cretaceous oceans - A 55 m.y. Record of Earth's temperature and carbon cycle, *Geology*, *40*, 107–110.

Goddéris, Y., Y. Donnadieu, V. Lefebvre, G. Le Hir, and E. Nardin (2014), The role of paleogeography in the Phanerozoic history of atmospheric CO_2 and climate, *Earth Sci. Rev.*, *128*, 122–138.

Gulbranson, E., N. Tabor, and I. Montañez (2011), A pedogenic goethite record of soil CO_2 variations as a response to soil moisture content, *Geochim. Cosmochim. Acta*, *75*, 7099–7116.

Hinnov, L., and J. Ogg (2007), Cyclostratigraphy and the astronomical time scale, *Stratigraphy*, *4*, 239–251.

Hönisch, B., G. Hemming, D. Archer, M. Siddall, and J. McManus (2009), Atmospheric carbon dioxide concentration across the mid-Pleistocene transition, *Science*, *324*, 1551–1554.

Hönisch, B., et al. (2012), The geological record of ocean acidification, *Science*, *335*, 1058–1063.

Intergovernmental Panel on Climate Change (2013), *Climate Change 2013: The Physical Science Basis. Contribution of Working Group I to the Fifth Assessment Report of the IPCC*, 1535 pp., Cambridge Univ. Press, Cambridge, U. K., and New York.

Kump, L., and M. Arthur (1999), Interpreting carbon-isotope excursions: Carbonates and organic matter, *Chem. Geol.*, *161*, 181–198.

Laskar, J., P. Robutel, F. Joutel, M. Gastineau, A. C. M. Correia, and B. Levrard (2004), A long-term numerical solution for the insolation quantities of the Earth, *Astron. Astrophys.*, *428*, 261–285.

Lefebvre, V., Y. Donnadieu, Y. Goddéris, F. Fluteau, and L. Hubert-Théou (2013), Was the Antarctic glaciation delayed by a high degassing rate during the early Cenozoic?, *Earth Planet. Sci. Lett.*, *371-372*, 203–211.

Littler, K., S. A. Robinson, P. R. Bown, A. J. Nederbragt, and R. D. Pancost (2011), High sea-surface temperatures during the Early Cretaceous Epoch, *Nat. Geosci.*, *4*, 169–172.

Lowenstein, T., M. Timofeeff, S. Brennan, L. Hardie, and R. Demicco (2001), Oscillations in phanerozoic seawater chemistry: Evidence from fluid inclusions, *Science*, *294*, 1086–1088.

Pagani, M., J. Zachos, K. Freeman, B. Tipple, and S. Bohaty (2005), Marked decline in atmospheric carbon dioxide concentrations during the paleogene, *Science*, *309*, 600–603.

Pagani, M., K. Caldeira, D. Archer, and J. Zachos (2006), An ancient carbon mystery, *Science*, *314*, 1556–1557.

Pagani, M., Z. Liu, J. LaRiviere, and A. C. Ravelo (2010), High Earth-system climate sensitivity determined from Pliocene carbon dioxide concentrations, *Nat. Geosci.*, *3*, 27–30.

Pälike, H., R. D. Norris, J. O. Herrle, P. A. Wilson, H. K. Coxall, C. H. Lear, N. J. Shackleton, A. K. Tripati, and B. S. Wade (2006), The heartbeat of the Oligocene climate system, *Science*, *314*, 1894–1898.

Passalia, M. G. (2009), Cretaceous pCO_2 estimation from stomatal frequency analysis of gymnosperm leaves of Patagonia, Argentina, *Palaeogeogr. Palaeoclimatol. Palaeoecol.*, *273*, 17–24.

Pucéat, E., C. Lécuyer, Y. Donnadieu, P. Naveau, H. Cappetta, G. Ramstein, B. T. Huber, and J. Kriwet (2007), Fish tooth $\delta^{18}O$ revising Late Cretaceous meridional upper ocean water temperature gradients, *Geology*, *35*, 107–110.

Retallack, G. (2001), A 300-million-year record of atmospheric carbon dioxide from fossil plant cuticles, *Nature*, *411*, 287–290.

Rickaby, R., E. Bard, E. Sonzogni, F. Rostek, L. Beaufort, S. Barker, G. Rees, and D. Schrag (2007), Coccolith chemistry reveals secular variations in the global ocean carbon cycle?, *Earth Planet. Sci. Lett.*, *253*, 83–95.

Royer, D. (2006), CO_2-forced climate thresholds during the Phanerozoic, *Geochim. Cosmochim. Acta*, *70*, 5665–5675.

Russon, T., D. Paillard, and M. Elliot (2010), Potential origins of 400–500 kyr periodicities in the ocean carbon cycle: A box model approach, *Global Biogeochem. Cycles*, *24*, GB2013, doi:10.1029/2009GB003586.

Sandberg, P. A. (1983), An oscillating trend in Phanerozoic non-skeletal carbonate mineralogy, *Nature*, *305*, 19–22.

Seki, O., G. L. Foster, D. N. Schmidt, A. Mackensen, K. Kawamura, and R. D. Pancost (2010), Alkenone and boron-based Pliocene pCO_2 records, *Earth Planet. Sci. Lett.*, *292*, 201–211.

Sexton, P., R. D. Norris, P. A. Wilson, H. Pälike, T. Westerhold, U. Röhl, C. T. Bolton, and S. Gibbs (2011), Eocene global warming events driven by ventilation of oceanic dissolved organic carbon, *Nature*, *471*, 349–352.

Wang, P., J. Tian, X. Cheng, C. Liu, and J. Xu (2004), Major Pleistocene stages in a carbon perspective: The South China Sea record and its global comparison, *Paleoceanography*, *19*, PA4005, doi:10.1029/2003PA000991.

Wang, P., J. Tian, and L. Lourens (2010), Obscuring of long eccentricity cyclicity in Pleistocene oceanic carbon isotope records, *Earth Planet. Sci. Lett.*, *290*, 319–330.

Zachos, J., M. Pagani, L. Sloan, E. Thomas, and K. Billups (2001), Trends, rhythms, and aberrations in global climate 65 Ma to present, *Science*, *292*, 686–693.

Zhang, Y., M. Pagani, Z. Liu, S. Bohaty, and R. DeConto (2013), A 40-million-year history of atmospheric CO_2, *Philos. Trans. R. Soc. A*, *371*, doi:10.1098/rsta.2013.0096.